Journal of Electrical and Computer Engineering Innovations
(JECEI)
Journal homepage: http://www.jecei.sru.ac.ir

Research paper

Design of a Microstrip Dual-Band Bandpass Filter Using Novel Loaded Asymmetric Two Coupled Lines for WLAN Applications

R. Salmani, A. Bijari*, S.H. Zahiri

Deptartment of Electrical Engineering, Faculty of Electrical and Computer Engineering, University of Birjand, Birjand, Iran.

Article Info

Article History:
Received 23 October 2019
Reviewed 02 December 2019
Revised 08 January 2020
Accepted 09 April 2020

Keywords:
Dual-band filter
Bandpass filter
Microstrip lines
Coupled lines
Transmission zeros

*Corresponding Author's Email Address:
a.bijari@birjand.ac.ir

Abstract

Background and Objectives: Due to the rapid development in wireless communications, bandpass filters have become key components in modern communication systems. Among the microwave filter technologies, planar structures of microstrip line are chosen, due to low profile, weight, ease of fabrication, and manufacturing cost.
Methods: This paper designs and simulates a new microstrip dual-band bandpass filter. In the proposed structure, three coupled lines and a loaded asymmetric two coupled line are used. The design method is based on introducing and generating the transmission zeros in the frequency response of a wideband single-band filter. A wideband frequency response is obtained using the three coupled lines, and the transmission zeros are achieved using the novel loaded asymmetric two coupled lines.
Results: The proposed dual-band filter is designed and simulated on a Rogers RO3210 substrate for WLAN applications. Dimension of the proposed filter is 11.22 mm × 13.04 mm. The electromagnetic (EM) simulation is carried out by Momentum EM (ADS) software. Simulation results show that the proposed dual-band bandpass filter has two pass-bands at 2.4 GHz and 5.15 GHz with a loss of less than 1 dB for two pass-bands.
Conclusion: Among the advantages of this filter, low loss, small size, and high attenuation between the two pass-bands can be mentioned.

Introduction

Microwave integrated circuits (MICs) and radio frequency integrated circuits (RFICs) require a filter to eliminate interference, select band, attenuate harmonics, or eliminate the modulation distortion caused by active circuits used in communication transceivers. The microstrip transmission lines are one of the most common planar transmission lines due to their simple construction using conventional lithography processes and easy integration with ICs. Microwave filters are used as essential elements in each communication system for discriminating the frequency components of interest from the unwanted ones. These filters play an essential role in the desired performance of the transceiver systems. Considering the advancements of wireless communication, the increase in bandwidth, and the development of new standards, small-sized microwave filters with excellent performance and low cost are required. Today, multiple band operation is considered to solve the insufficient capacity of the communication systems. Thus, new microwave filters should be able to operate in two or more non-harmonic frequency bands. With the development of wireless communication standards in the ultra-wideband context, filters that can operate in two or more frequency ranges, like IEEE806.16, IEEE806.11, CDMA, and GSM are required [1]. The components of the dual-band or multiple band bandpass filter can be used to meet this requirement. Almost all bands that are used for commercial purposes are very close in terms of position and bandwidths. For example, WiFi, WiMAX, and GSM systems operate in the frequency bands of 0.9-1.8 GHz, 2.4-2.45 GHz, 3.5 GHz and 5.2-5.25 GHz. Since 1997 with the approval of using wireless local area networks (WLAN) for commercial purposes, applications of this technology have grown quickly. According to IEEE 802.11a/b/g, WLAN is applied in the frequency bands of 2.4-2.45 GHz, and 5.2-5.25 GHz. Considering the performance of dual-band and multiple-band filters in the stop-band, their size and construction cost, their design is very challenging. Since achieving excellent characteristics for close pass-bands is difficult, recently, various methods and structures have been proposed to develop the novel flat multiple-band filters, like designing the filter in classic form, using multi-mode resonators (MMR), and introducing and generating transmission zeros in the frequency response of a wideband single-band filter. In [2], a dual-band bandpass filter using open-circuit and short-circuit loaded stubs has been designed and simulated. The proposed dual-band filter includes a second-order bandpass filter and a third-order bandpass filter, which are designed independently. The characteristics of the dual-band filter are obtained by combining two single-band bandpass filters that increases the filter dimension. Another limitation of the scheme is the short-circuit using via to ground. The bandwidth of the pass-bands can be controlled using impedance and length of the stubs. In [3], a novel microstrip dual-band filter with excessive loss in the stop-band has been introduced. The structure of the proposed filter includes coupled transmission lines and radial stubs. A dual-band bandpass filter using a novel microstrip dual-mode resonator based on a split-loop rectangular resonator with an open-circuit stub loaded has been presented in [4]. The proposed filter is based on the cross-coupling of a pair of modified resonators. The first higher order spurious mode is located at about 6 GHz, which limits the higher stopband width. In [5], a dual-band bandpass filter using a five-mode resonator has been proposed. The first three resonance modes are used for the first pass-band, and the two other modes are used for the second pass-band. Although the filter proposed has employed a five-mode resonator, using five open-circuit loaded stubs to achieve this goal increases the proposed filter's dimensions. A simple and effective method for designing the dual-band bandpass filters with high isolation and wide stop-band using open-circuit resonators loaded with one stub has been presented in [6]. The proposed structure is based on the conventional stub loaded resonator (SLR) that increases the filter dimension. In [7], two cells have been presented for implementation in passive circuits with a wide stop-band. Both cells include step impedance resonators and DGS structures. Based on these two cells, two dual-band bandpass filters have been designed and constructed. Using this cells and cascade them to achieve the characteristics of a dual-band filter increases the filter's dimension. Two single-band and dual-band microstrip bandpass filters with source and load loaded with dual-mode ring resonators based on two-layer structures have been presented in [8]. In this study, the proposed filter is introduced based on introducing and generating transmission zeros in the frequency response of the wideband single-band filter for WLAN applications. A wideband frequency response is realized using the three coupled lines, and the novel loaded asymmetric two coupled lines are used to generate the transmission zeros in the wideband frequency response.

Filter Design

A. Three coupled lines

If two or more transmission lines are very close to each other, the power is coupled between two lines due to interference of EM fields. Such lines are known as coupled transmission lines comprised of two conductors that are very close, although more conductors can be used. It is usually assumed that the coupled transmission lines are in TEM mode, valid for strip structures and microstrip structures. Fig. 1 (a) shows a parallel symmetric three coupled microstrip line with distance s. If the TEM mode is considered, the electrical characteristics of the coupled lines can be described by measuring the effective capacitances between the lines and the propagation speed on the line. According to the transmission theory, a transmission line can be modeled as a capacitance, inductance, and resistance. A three coupled structure supports three pseudo-TEM modes called a, b, and c [9]. To obtain the coupled structure's parameters, it is sufficient to obtain the capacitive matrix [C] per unit length. The symmetric three coupled microstrip lines provide two transmission zeros at f=0 and $f=2f_0$. In this study, three coupled microstrip lines are used instead of the conventional two coupled lines, which increases the coupling and fractional bandwidth. In this case, the current of ports 1, 3, and 5 is zero, and its transmission matrix is described based on the width of the lines and their distance [9]. The equivalent circuit of the three coupled line is shown in Fig. 1 (b).

B. Introducing a New Resonator

In this study, a new resonator is presented using loaded asymmetric two coupled lines, as shown in Fig. 2.

This new open-circuit resonator comprises an asymmetric two coupled line with characteristic impedance of $Z_{0\pi}$ and Z_{0C} with an electrical length of ϑ_1 and a loaded line with characteristic impedance of Z_2, and electrical length of ϑ_2. For the asymmetric two coupled structure, the relationship of the four-port network, its voltages and impedance parameters are represented in the following matrix form.

$$[V]_{4\times1} = [Z]_{4\times4}[I]_{4\times1} \tag{1}$$

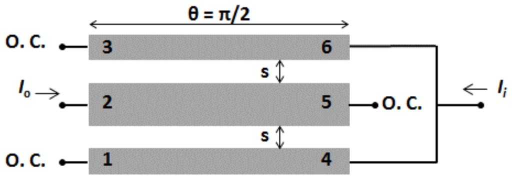

(a)

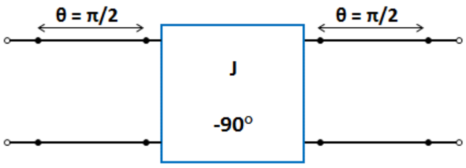

(b)

Fig. 1: (a) three coupled line, (b) its equivalent circuit.

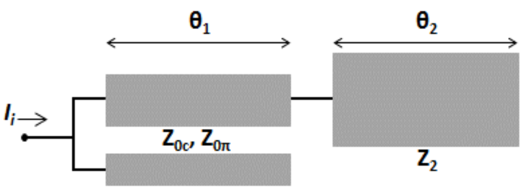

Fig. 2: The proposed new resonator.

The asymmetric two coupled line supports two pseudo-TEM propagation modes known as c and π. To obtain the parameters of the coupled structure, it is sufficient to obtain the capacitive matrix [C] per unit length.

The open-circuit impedance matrix of this four-port network can be obtained considering the superposition of modes c and π. The elements of the open-circuit impedance matrix [Z] are as follows [10]:

$$Z_{11} = Z_{33} = -j\left[\frac{Z_{01c}\cot\theta_c}{(1-R_c/R_\pi)} + \frac{Z_{01\pi}\cot\theta_\pi}{(1-R_\pi/R_c)}\right] \tag{1-2}$$

$$Z_{12} = Z_{21} = Z_{34} = Z_{43} = -j\left[\frac{Z_{01c}R_c\cot\theta_c}{(1-R_c/R_\pi)} + \frac{Z_{01\pi}R_\pi\cot\theta_\pi}{(1-R_\pi/R_c)}\right] \tag{2-2}$$

$$Z_{14} = Z_{41} = Z_{23} = Z_{32} = -j\left[\frac{Z_{01c}R_c}{(1-R_c/R_\pi)\sin\theta_c} + \frac{Z_{01\pi}R_\pi}{(1-R_\pi/R_c)\sin\theta_\pi}\right] \tag{3-2}$$

$$Z_{13} = Z_{31} = -j\left[\frac{Z_{01c}}{(1-R_c/R_\pi)\sin\theta_c} + \frac{Z_{01\pi}}{(1-R_\pi/R_c)\sin\theta_\pi}\right] \tag{4-2}$$

$$Z_{22} = Z_{44} = -j\left[\frac{Z_{01c}R_c^2\cot\theta_c}{(1-R_c/R_\pi)} + \frac{Z_{01\pi}R_\pi^2\cot\theta_\pi}{(1-R_\pi/R_c)}\right] \tag{5-2}$$

where ϑ_c and ϑ_π are the electric length of the asymmetric two coupled transmission line in mode c and mode π. The equations governing the electric length of the line are as follows: $\theta = \beta l$ that $\beta = \frac{2\pi}{\lambda_g}$ and $\lambda_g = \frac{c}{f_0\sqrt{\varepsilon_{re}}}$. Where l is the physical length of the line, β is the propagation constant, λ_g is the wavelength, and ε_{re} is the effective dielectric constant of the line. Z_{01C} and $Z_{01\pi}$ are the characteristic impedance of line 1, R_C and R_π are the parameters of the two excitation modes that are obtained using the capacitance per unit length. The Z_{01C}, $Z_{01\pi}$, R_C and R_π are defined in Appendix. Fig. 3 shows the asymmetric two coupled microstrip line used in the proposed resonator. This asymmetric coupled line operates as a band stop filter. The input is taken by connecting ports 1 and 2, and the output is taken from ports 3, while the ports 4 is open-circuit. "Equation (3)" describes the equivalent coupling line conditions:

$$I_4 = 0 \tag{1-3}$$

$$I_1 + I_2 = I_i \tag{2-3}$$

$$V_1 = V_2 = V_i \tag{3-3}$$

$$V_3 = V_o \tag{4-3}$$

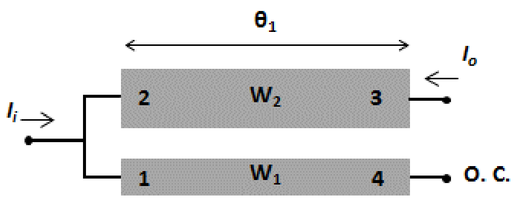

Fig. 3: The proposed structure using the asymmetric two coupled lines.

By applying the equivalent coupled line conditions in "(1)", we have:

$$V_i = Z_{11}I_1 + Z_{12}(I_i - I_1) + Z_{13}I_o \tag{1-4}$$

$$V_i = Z_{12}I_1 + Z_{22}(I_i - I_1) + Z_{14}I_o \quad (2\text{-}4)$$

$$V_o = Z_{13}I_1 + Z_{14}(I_i - I_1) + Z_{11}I_o \quad (3\text{-}4)$$

$$V_4 = Z_{14}I_1 + Z_{24}(I_i - I_1) + Z_{12}I_o \quad (4\text{-}4)$$

Therefore, by solving these equations, the impedance matrix of the equivalent two-port network is obtained using the following equations:

$$\begin{bmatrix} V_i \\ V_o \end{bmatrix} = \begin{bmatrix} Z'_{11} & Z'_{12} \\ Z'_{21} & Z'_{22} \end{bmatrix} \begin{bmatrix} I_i \\ I_o \end{bmatrix} \quad (5)$$

where

$$Z'_{11} = \frac{Z_{11}Z_{22} - Z_{12}^2}{Z_{11} - 2Z_{12} + Z_{22}} \quad (1\text{-}6)$$

$$Z'_{12} = Z'_{21} = \frac{Z_{11}Z_{14} - Z_{12}Z_{13} - Z_{12}Z_{14} + Z_{13}Z_{22}}{Z_{11} - 2Z_{12} + Z_{22}} \quad (2\text{-}6)$$

$$Z'_{22} = \frac{Z_{11}^2 - 2Z_{11}Z_{12} + Z_{11}Z_{22} - Z_{13}^2 + 2Z_{13}Z_{14} - Z_{14}^2}{Z_{11} - 2Z_{12} + Z_{22}} \quad (3\text{-}6)$$

The parameters of the above impedance matrix can be calculated using "(2)". By converting the impedance parameters of the dual network to transmission parameters of ABCD, we have [10]:

$$A = \frac{\cos\theta_c \cos\theta_\pi (R_c - R_\pi)}{R_c(1-R_\pi)\cos\theta_\pi - R_\pi(1-R_c)\cos\theta_c} \quad (1\text{-}7)$$

$$C = \frac{j}{R_c(1-R_\pi)\cos\theta_\pi - R_\pi(1-R_c)\cos\theta_c} \left[\frac{(1-R_c)^2\cos\theta_c}{R_c Z_{01\pi}\csc\theta_\pi} - \frac{(1-R_\pi)^2\cos\theta_\pi}{R_\pi Z_{01c}\csc\theta_c} \right] \quad (2\text{-}7)$$

$$\begin{aligned} D = {} & \{\cos\theta_c \cos\theta_\pi \left[R_\pi^2(1-R_c)^2 + R_c^2(1-R_\pi)^2 \right] \\ & + R_c R_\pi \sin\theta_c \sin\theta_\pi \left[\frac{Z_{01c}}{Z_{01\pi}}(1-R_c)^2 + \frac{Z_{01\pi}}{Z_{01c}}(1-R_\pi)^2 \right] \\ & - 2R_c R_\pi (1-R_c)(1-R_\pi)\} / (R_c - R_\pi) \\ & \left[R_c(1-R_\pi)\cos\theta_\pi - R_\pi(1-R_c)\cos\theta_c \right] \end{aligned} \quad (3\text{-}7)$$

$$B = \frac{1}{C}(AD - 1) \quad (4\text{-}7)$$

In "(7)," it is assumed that the electrical length of the line for both modes are equal ($\vartheta_1=\vartheta_C=\vartheta_\pi$). In Fig. 2, the transmission matrix of ABCD is obtained as the product of the two coupled line's transmission matrices and the open-circuit stub loaded. The transmission matrix of the equivalent dual line is represented with $[ABCD]_1$, which is extracted from "(7)". The transmission matrix of the loaded line is represented with $[ABCD]_2$. Thus:

$$\begin{bmatrix} A & B \\ C & D \end{bmatrix} = \begin{bmatrix} A_1 & B_1 \\ C_1 & D_1 \end{bmatrix} \begin{bmatrix} A_2 & B_2 \\ C_2 & D_2 \end{bmatrix} \quad (8)$$

where

$$\begin{bmatrix} A_2 & B_2 \\ C_2 & D_2 \end{bmatrix} = \begin{bmatrix} \cos\theta_2 & jZ_2\sin\theta_2 \\ \dfrac{j\sin\theta_2}{Z_2} & \cos\theta_2 \end{bmatrix} \quad (9)$$

Considering the definition of the transmission matrix as follows:

$$\begin{bmatrix} V_i \\ I_i \end{bmatrix} = \begin{bmatrix} A & B \\ C & D \end{bmatrix} \begin{bmatrix} V_o \\ -I_o \end{bmatrix} \quad (10)$$

The input impedance of the equivalent network of Fig. 2, is calculated using the following equation, assuming that the two lines are of the same length ($\vartheta_1=\vartheta_2\cong\pi/2$). It should be noted that the stub loaded is open-circuit (I_o=0).

$$\begin{aligned} Z_i = {} & -\{jR_\pi \cot\theta[Z_2\cos^2\theta(R_c - R_\pi) \\ & + R_c R_\pi \sin^2\theta(R_c Z_{01c} - R_\pi Z_{01\pi})] \\ & R_c Z_{01c} Z_{01\pi}(R_c - R_\pi)\} / \{[2R_c R_\pi Z_{01c}\csc\theta \\ & ((R_\pi^2 - R_\pi + \tfrac{1}{2})R_c^2 - R_c R_\pi^2 + \tfrac{1}{2}R_\pi^2) Z_{01\pi}\sin\theta \\ & + Z_2(R_c^2 R_\pi Z_{01c} + (-R_\pi^2 Z_{01\pi} + (-2Z_{01c} \\ & + 2Z_{01\pi})R_\pi - Z_{01\pi})R_c + R_\pi Z_{01c})(R_c - R_\pi)]\cos^2\theta \\ & + R_c^2 R_\pi^2((R_c^2 Z_{01c}^2 + R_\pi^2 Z_{01\pi}^2 - 2R_c Z_{01c}^2 - 2R_\pi Z_{01\pi}^2 \\ & + Z_{01c}^2 + Z_{01\pi}^2)\sin^2\theta - 2Z_{01c}Z_{01\pi}(R_\pi - 1)(R_c - 1))\} \end{aligned} \quad (11)$$

For resonance, when Z_{in} is zero, by calculating ϑ for assumed R_π and R_C, the transmission zeros' location can be obtained using the following equations:

$$\theta = \begin{cases} \tan^{-1}\left(\sqrt{\dfrac{2NR}{R+1}}\right. \\ \dfrac{\pi}{2} \end{cases} \quad (12)$$

where

$$R = \frac{Z_{01c}}{Z_{01\pi}} \quad (1\text{-}13)$$

$$N = \frac{Z_2}{Z_{01c}} \quad (2\text{-}13)$$

If is defined at the central frequency of f_0, then the relationship between R and location of the transmission zeros for different values of N is calculated using Fig. 4. In all cases, three transmission zeros resulting from length, quarter wavelength at the central frequency of f_0 are shown.

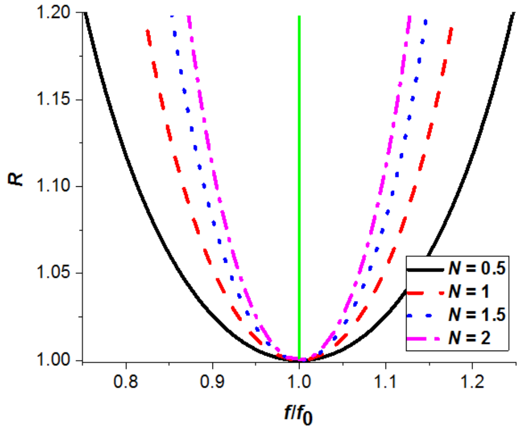

Fig. 4: Variations of the location of the transmission zeros vs. *R* for different values of *N*.

C. Implementation

In this paper, the initial design starts with a third-order elliptical bandpass filter and a ladder circuit equivalent to the lumped elements. Then, admittance inverters (*J*) are used to approximate the lumped elements to the distributed elements. An ideal admittance inverter is a two-port network in which the input admittance is equal to the inverse load admittance. Thus, it can be used to convert the series elements to parallel elements and vice versa. An admittance inverter can be constructed using a quarter-wave converter with proper characteristic impedance. The Schematic of the generalized proposed dual-band filter is shown in the following Fig. 5 (a). The proposed dual-band bandpass filter is shown in Fig. 5 (b). The proposed filter includes a symmetric three coupled microstrip line and loaded asymmetric two coupled microstrip line.

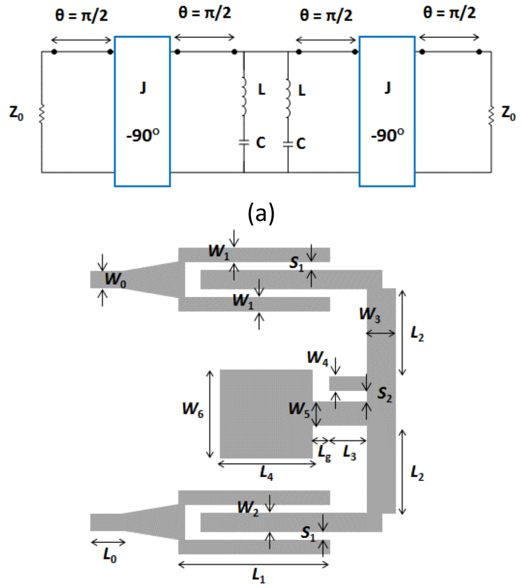

Fig. 5: (a) Schematic of the generalized proposed dual-band filter (b) The proposed dual-band filter.

Results and Discussion

The proposed dual-band microstrip filter shown in Fig. 5 (b), is designed and simulated on a Rogers RO3210 substrate with the thickness of 0.64 mm. The dielectric constant is 10.2, and the loss tangent is 0.0027. The proposed structure is simulated and optimized using momentum in ADS, as shown in Fig. 6. The dimensions after optimization are list in Table 1.

Table 1: Dimentsions of the proposed filter (milimeter)

W_0	W_1	W_2	W_3	W_4
0.58	0.33	0.27	1.05	0.20
W_5	W_6	S_1	S_2	L_0
1.80	4.85	0.12	0.10	0.75
L_1	L_2	L_3	L_4	L_g
7.65	4.75	0.32	4.80	0.50

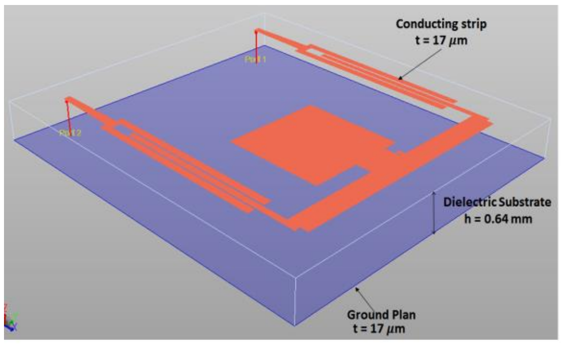

Fig. 6: Simulation of the proposed filter in Momentum ADS.

The frequency response of the proposed filter is shown in Fig. 7.

The proposed filter includes two pass-bands at the central frequencies of 2.4 GHz and 5.15 GHz with fractional bandwidths of 22.9% and 15.5%. The maximum insertion losses and the return losses in the first band are 0.5 dB and 11 dB, and they are 1 dB and 9 dB in the second band.

Also, there is one transmission zero between the two pass-bands at the frequency of 3.68 GHz with maximum attenuation of 49.5 dB.

Dimension of the proposed filter is 11.22 mm × 13.04 mm or 0.23 λ_g × 0.27 λ_g, where λ_g is the wavelength of the 50-Ω microstrip line over the substrate at central frequency of the first passband (2.4 GHz).

The input and output of the proposed filter are terminated with an impedance of Z_0=50 Ω. Therefore, the width of the feedlines (W_0=0.58 mm) are designed to provide matching with the characteristic impedance of 50 Ω.

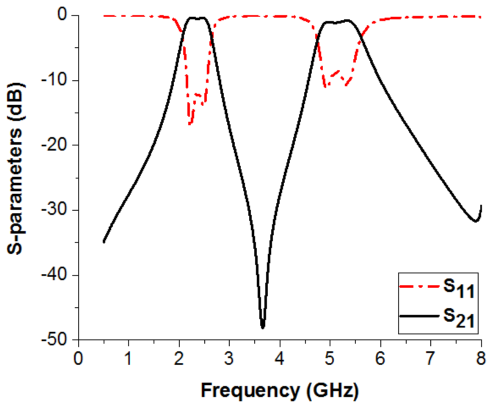

Fig. 7: Frequency response of the proposed filter.

In the following figure, the frequency response of the proposed filter is evaluated by the termination resistors of 25 Ω and 75 Ω. As can be seen, any mismatch at the circuits' input and output connected to the feed lines of the proposed filter can degrade the insertion loss at two frequency bands, particularly the second passband. As can be seen in Table 2, the proposed filter exhibits better insertion loss at the central frequencies, particularly at the first passband. Although the insertion loss of the filter in [2] is almost the same as the proposed filter, but its dimensions is 24.4 mm×17.5 mm, which is larger than the proposed filter.

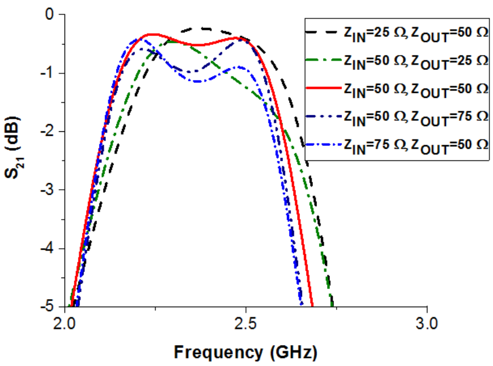

(a)

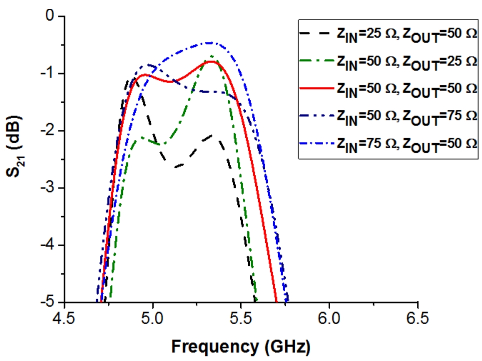

(b)

Fig. 8: Effect of termination resistors mismatch on the frequency response of the proposed filter at the (a) lower band (b) upper band.

Conclusion

This study presents the design, simulation, and optimization of a flat microstrip dual-band filter with symmetric three coupled lines and asymmetric two coupled lines. The proposed filter is designed for wireless local area networks (WLAN) with two pass-bands at the frequencies of 2.4 GHz and 5.15 GHz. The proposed filter has a maximum insertion loss of 0.5 dB and 1 dB and a return loss of 11 dB and 9 dB for the first and second pass-bands.

The proposed filter is designed and modeled systematically. This filter can also be implemented on a Rogers substrate with small dimensions of 11.22 mm × 13.04 mm or 0.23 λg × 0.27 λg, λg is the wavelength at the central frequency of the first pass-band.

The proposed filter could thus be a good choice for multiband receivers.

Author Contributions

R. Salmani and A. Bijari developed the theoretical idea and performed the analytic calculations. R. Salmani carried out the simulations. All authors discussed the results and contributed to the final manuscript. A. Bijari and S. H. Zahiri supervised the project.

Acknowledgment

We thank our colleagues from the university of Birjand who provided insight and expertise that greatly assisted the research. We thank M. Forouzanfar assistance for comments that greatly improved the manuscript.

Conflict of Interest

The author declares that there is no conflict of interests regarding the publication of this manuscript. In addition, the ethical issues, including plagiarism, informed consent, misconduct, data fabrication and/or falsification, double publication and/or submission, and redundancy have been completely observed by the authors.

Abbreviations

WLAN	Wireless Local Area Network
MICs	Microwave Integrated Circuits
RFICs	Radio Frequency Integrated Circuits
CDMA	Code Division Multiple Access
GSM	Global System for Mobile
WiFi	Wireless Local Area Network Product Based on the IEEE 802.11
WiMAX	Worldwide Interoperability for Microwave Access
MMR	Multi Mode Resonator
EM	Electromagnetic
TEM	Transverse Electromagnetic mode

Table 2: Comparison of the proposed filter with its dual-band counterparts

Ref.	f_{01} (GHz)	f_{02} (GHz)	IL_{01} (dB)	IL_{02} (dB)	RL_{01} (dB)	RL_{02} (dB)	Size ($\lambda_g \times \lambda_g$)	Size(mm×mm)
[2]	2.4	5.2	0.3	0.7	22.1	20.8	0.28 × 0.20	24.4×17.5
[4]	2.12	3.91	0.92	2.11	17.3	15.4	0.24 × 0.18	26.4×20.3
[6]	3.5	5.25	1.87	2.33	>20	>20	0.459 × 0.323	27×19
[7] Filter A	3.17	3.91	1.76	1.63	>20	>20	0.389 × 0.177	27×12.5
[7] Filter B	3.16	3.90	1.87	1.67	>18	>20	0.385 × 0.213	26.9×14.75
[11] Filter A	1.8	5.8	1.33	1.7	21	13	0.23×0.17	28×20.5
[11] Filter B	2.4	5.8	1.35	1.97	17	15	0.39×0.25	35×22.5
[12]	2.82	3.21	1.9	1.7	21.6	16.1	2.76 × 1.30	21.4×10.1
[13]	3.78	4.82	1.38	1.82	14	33	0.16 × 0.31	-
This work	2.4	5.15	0.5	1	11	9	0.23 × 0.27	11.22×13.04

Appendix

The asymmetric two coupled line supports two pseudo-TEM propagation modes known as c and π. To obtain the parameters of the coupled structure, it is sufficient to obtain the capacitive matrix [C] per unit length. The phase velocity $v_{C,\pi}$ and the voltage ratio of the two lines $R_{C,\pi}$ are obtained from the following relations:

$$v_{c,\pi} = \left[\frac{D_1+D_2}{2} \pm \frac{1}{2}\sqrt{(D_1-D_2)^2+4E_1E_2}\right]^{-1/2} \quad (1\text{-}14)$$

$$R_{c,\pi} = \frac{1}{2E_1}\left[(D_2-D_1) \pm \sqrt{(D_2-D_1)^2+4E_1E_2}\right] \quad (2\text{-}14)$$

where

$$D_1 = (C_{11}C_{022} - C_{12}C_{012})/(v_0^2 \det[C_0]) \quad (1\text{-}15)$$

$$D_2 = (C_{22}C_{011} - C_{12}C_{012})/(v_0^2 \det[C_0]) \quad (2\text{-}14)$$

$$E_1 = (C_{12}C_{022} - C_{22}C_{012})/(v_0^2 \det[C_0]) \quad (3\text{-}14)$$

$$E_2 = C_{12}C_{011} - C_{012}^2 \quad (4\text{-}14)$$

$$[C_0] = C_{011}C_{022} - C_{012}^2 \quad (6\text{-}14)$$

where v_0 is the phase velocity in free space. The impedance of the i-th line in the j-th mode Z_{0ij} can be obtained from the following equations:

$$Z_{01j} = \frac{1}{v_j(C_{11}+R_jC_{12})} \quad (1\text{-}16)$$

$$Z_{02j} = \frac{1}{v_j(C_{22}+R_j^{-1}C_{12})} \quad (2\text{-}16)$$

The elements of the open-circuit impedance matrix [**Z**] are given in "(2)".

References

[1] V.C. Benjin, Advances in Multi-Band Microstrip Filters, Cambridge university press, 2015.

[2] G. Liang, F. Chen, "A Compact Dual-Wideband Bandpass Filter Based on Open-/Short-Circuited Stubs," IEEE Access, 8: 20488-20492, 2020.

[3] H. Abasi, A.R. Hazeri, "Compact microstrip dual-narrowband bandpass filter with wider rejection band," Electromagnetics, 38(6): 390–401, 2018.

[4] H. Chen, K. Chen, X. Chen, "Planar dual-mode dual-band bandpass filter using a modified rectangular split-loop resonator loaded by an open-circuited stub," Journal of Electromagnetic Waves and Applications, 30: 1964-1973, 2016.

[5] C.F. Chen, G.Y. Wang and J.J. Li, "Compact microstrip dual-band bandpass filter and quad-channel diplexer based on quint-mode stub-loaded resonators," IET Microwaves, Antennas & Propagation, 12: 1913-1919, 2018.

[6] Y. Xie, F.C. Chen, Z. Li, "Design of Dual-Band Bandpass Filter with High Isolation and Wide Stopband," IEEE Access, 5: 25602-25608, 2017.

[7] Y. Rao, H.J. Qian, B. Yang, R.G. Garcia, X. Luo, "Dual-Band Bandpass Filter and Filtering Power Divider with Ultra-Wide Upper Stopband Using Hybrid Microstrip/DGS Dual-Resonance Cells," IEEE Access, 8: 23624-23637, 2020.

[8] Q. Liu, D. Zhang, J. Zhang, D. Zhou, N. An, "Compact single- and dual-band bandpass filters with controllable transmission zeros using dual-layer dual-mode loop resonators," 14: 522-531, 2020.

[9] R. Schwindt, C. Nguyen, "Spectral Domain Analysis of Three Symmetric Coupled Lines and Application to a New Bandpass Filter," IEEE Transactions on Microwave Theory and Techniques, 42(7): 1183-1189, 1994.

[10] C. Nguyen, K. Chang, "On the Analysis and Design of Spurline Bandstop Filters," IEEE Transactions on Microwave Theory and Techniques, 33(12): 1416-1421, 1985.

[11] Z. C. Zhang, Q. X. Chu, F. C. Chen, "Compact Dual-Band Bandpass Filters Using Open-/Short-Circuited Stub-Loaded λ/4 Resonators," IEEE Microwave and Wireless Components Letters, 25(10): 657-659, 2015.

[12] R. Gomez-Garcia, J.-M. Munoz-Ferreras, W. Feng, D. Psychogiou, "Balanced symmetrical quasi-reflectionless single-and dual-band band- pass planar filters," IEEE Microwave Wireless Component Letter, 28(9): 798-800, 2018.

[13] L. T. Wang, Y. Xiong, L. Gong, M. Zhang, H. Li, X.-J. Zhao, "Design of dual-band bandpass filter with multiple transmission zeros using transversal signal interaction concepts," IEEE Microwave Wireless Component Letter, 29(1): 32-34, 2019.

Biographies

Reza Salmani received the BS degrees, in Telecommunications engineering and MSc degrees in Electronics engineering from University of Birjand, Iran, in 2014, and 2016, respectively. Currently, he is PhD Student, University of Birjand, Iran. Research interests: Microwave filters.

Abolfazl Bijari was born in Birjand, Iran in 1982. He received M.S. and Ph.D. in Electronics Engineering from Ferdowsi University of Mashhad (FUM), Iran in 2007 and 2013, respectively. He also took part in a year joint collaboration at the Synchrotron Light Research Institution (SLRI), in 2011 where he worked on LIGA-based micromechanical resonators. His research interest includes RF-MEMS, and RF circuit design for wireless communications. He is currently an Assistant Professor of Electrical Engineering at the University of Birjand.

Seyed Hamid Zahiri received the BS, MSc and PhD degrees in Electronics Engineering from Sharif University of Technology, Tehran, Iran, Tarbiat Modarres University, Tehran, and Ferdowsi University of Mashhad, Iran, in 1993, 1995, and 2005, respectively. Currently, he is a Professor in the Department of Electronics Engineering, University of Birjand, Iran. His research interests include pattern recognition, swarm intelligence algorithms, AI, and evolutionary algorithms.

How to cite this paper:

R. Salmani, A. Bijari, S.H. Zahiri, "Design of a microstrip dual-band bandpass filter using novel loaded asymmetric two coupled lines for WLAN applications," Journal of Electrical and Computer Engineering Innovations, 8(2): 255-262, 2020.

DOI: 10.22061/JECEI.2020.7250.376

URL: http://jecei.sru.ac.ir/article_1469.html